Proceedings of the 12th Laser Applications Forum
November 23-24, 2022
Congress Centrum Bremen

Influence of powder feed parameters on the powder stream in laser metal deposition (LMD) by high-speed and high-resolution imaging

Annika Bohlen*[1], Dieter Tyralla[1], Thomas Seefeld[1]

[1] BIAS – Bremer Institut für angewandte Strahltechnik GmbH, Klagenfurter Straße 5, 28359 Bremen, Germany

Abstract

Laser metal deposition (LMD) is a blown powder process used for the additive manufacturing of large components or the generation of functional geometries on semi-finished parts. In LMD laser intensity and powder mass flow distribution within the process zone must be precisely matched for a welding bead of predefined shape and a consistent layer quality. Therefore, the present work analyses the powder stream of a single injector that is commonly used for discrete coaxial nozzles in LMD. Several powder size classes are investigated in a range of 45 µm and 106 µm. The influence of carrier gas flow rate and powder mass flow rate variations on powder stream characteristics like particle velocity and propagation were determined up to a distance of 10 mm from the nozzle by high-speed imaging at a frequency of 30 kHz with a high spatial resolution. It was found that particle velocity depends mainly on carrier gas flow rate and particle size. Additionally, the measurement shows that the divergence increases for higher distances and higher particle sizes.

Keywords: Laser Metal Deposition, Powder-Jet, High-Speed Imaging

1 Introduction

Additive manufacturing is a production technology with increasing importance for metallic component production. Not only prototypes can be additively built, also the number of additively built end products increases steadily. Laser metal deposition (LMD) utilizes blown powder, making it a freeform process. This brings advantages for the achievable size of components, compared to other laser additive processes. The achievable geometric resolution and build rate are highly dependent on the powder supply to the process zone. Due to the extensive developments in the past decades, numerous different system technologies for powder feeding and powder nozzles have been established on the market. In general, the powder feed systems are differentiated into lateral and coaxial systems.

The importance of the powder stream characteristics in LMD is already addressed in many studies. Prasad et al. showed that a powder stream that is well-focused to the melt pool does not only lead to a better catchment efficiency but can also lead to better geometrical tolerances [1]. A lower velocity of the particles, as well as lower particle size and higher bonding temperature are beneficial for a better catchment efficiency [2]. An increase in carrier gas flow rate leads to a higher divergence of the powder stream, as well as to a decrease of powder concentration [3]. Additionally, a high carrier gas flow rate can lead to an increased spatter generation during the deposition process [4]. Balu et al. showed that the density, shape, and diameter of powder particles play a key role for stable powder flows [5]. Smurov et al. investigated the influence of particle size on the divergence for annular gap nozzles. Their model shows a strong increase in divergence with a particle size increase from 20 µm to 80 µm [6].

Previous work took a detailed look at the influence of wall roughness on the simulation of particle propagation behavior [7], as well as at the powder propagation behavior on a macroscopic scale [8]. This paper presents a high-speed and high-resolution imaging technique to gain a detailed insight into powder stream be-

*E-mail address of corresponding author: bohlen@bias.de

Edited by Thomas Seefeld, Tim Radel, Thorsten Mattulat
Available online at https://doi.org/10.26092/elib/1871; In: Proceedings of the 12th Laser Applications Forum, Strahltechnik, Band 76, ISBN 978-3-933762-70-2

havior, with the ability to automatically trace thousands of particles and measure their velocity and divergence. Different particle fractions were examined to obtain a deeper understanding of the influence of particle size on the powder stream behavior.

2 Experimental

2.1 Material

Stainless steel 316L powder material was used with a powder size of 45 µm to 106 µm according to the manufacturer. The sieve analysis from the manufacturer can be found in Tab. 1. The powder was sieved before experiments using the following mesh sizes: 45 µm, 53 µm, 63 µm, 71 µm, 80 µm, 90 µm, 100 µm and 106 µm, resulting in nine different size fractions. Of the seven used fractions, a SEM picture was taken to evaluate fraction specific morphologies (see Fig. 1).

Tab. 1: Sieve analysis from powder manufacturer.

< 38 µm (%)	38 µm – 45 µm (%)	45 µm – 53 µm (%)	53 µm – 63 µm (%)	63 µm – 90 µm (%)	90 µm – 106 µm (%)	106 µm – 125 µm (%)	> 125 µm (%)
0.0	1.7	15.5	16.5	49.3	16.9	0.1	0.0

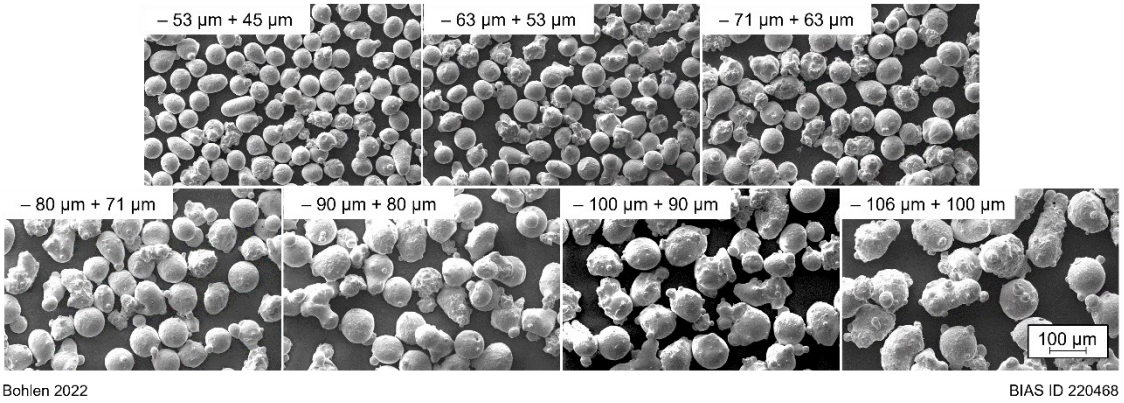

Fig. 1: SEM images of each sieved powder fraction.

2.2 Setup and Analysis Method

A powder feeder from Oerlikon Metco (type TWIN-150) was used. The powder was fed using Argon as carrier gas with variable gas flows. A single jet powder nozzle was used for these studies, which was vertically directed. The nozzle consists of a ceramic inner tube with a copper outer shielding. The opening has a diameter of 1.7 mm. The powder mass flow rate was varied between 1 g/min and 6 g/min with a constant carrier gas flow rate of 2.5 l/min. The carrier gas flow rate was varied between 1 l/min and 5 l/min with a constant powder mass flow rate of 3 g/min. A high-speed camera (Vision Phantom Research VEO410L) was used to observe the particle flow in combination with an illumination laser (Cavitar Cavilux HF). The illumination laser was directed at a white sheet of paper behind the powder flow to achieve a high contrast between powder particles and background, see Fig. 2.

All high-speed videos were recorded at 30 kHz with an image size of 384 px × 376 px. One pixel width is equivalent to 26.27 µm. Each parameter set was recorded in at least 13,000 frames, this equals 433.3 ms. A LabView based program was used to analyze the obtained videos. From the first 5,000 frames a background model was created by calculating a mean frame. For each frame the background model was used to calculate the absolute difference. This image was then binarized and used for particle detection. Particles from each frame were then searched in the next frame. If they could be detected the distance between the particles in the frames was measured. Thus, particles were traced through multiple frames, making it possible to gain a mean velocity per particle and counting unique particles. See Fig. 2 for an exemplary analysis of one frame.

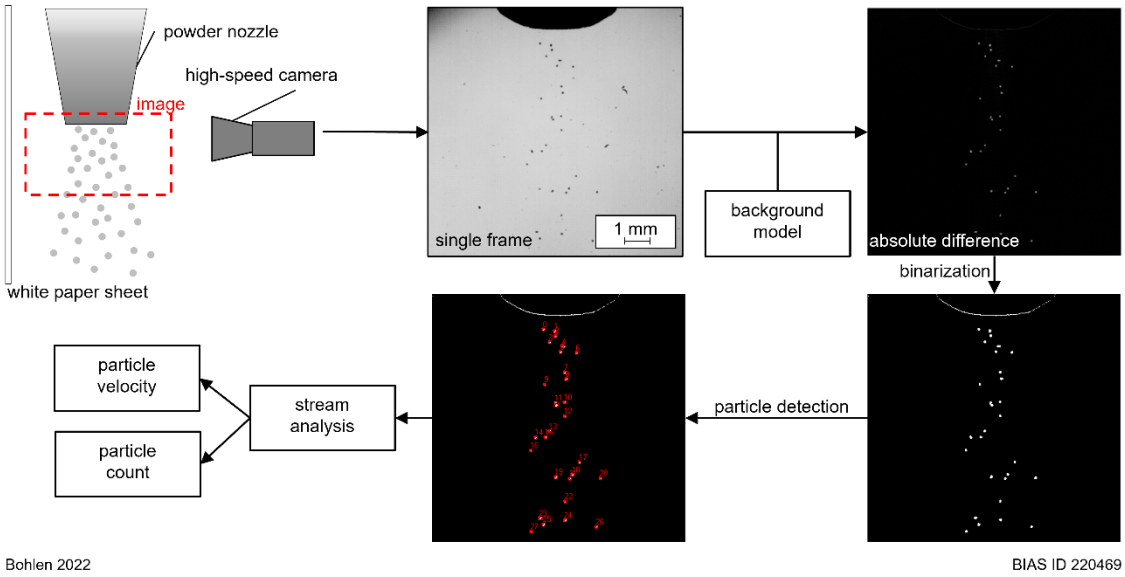

Fig. 2: Sketch of the experimental setup for high-speed imaging and exemplary analysis of one frame.

3 Results and Discussion

Fig. 3 shows the counted particles for the varied powder mass flow rate for each of the sieved particle fractions. The background coloration shows the theoretical number of particles for each fraction, calculated for ideal spheres, over a conveying time of 433.3 ms. The counted particles from the high-speed videos are in good accordance with the calculated amounts, except for the particle classes 45 µm – 53 µm and 100 µm – 106 µm.

An explanation as to why the biggest fraction differs to calculated values can be found in the shape of the particles. Fig. 1 shows that the particles in the faction from 100 µm to 106 µm show defects in respect to their shape being more elongated than in the other fractions. During sieving these elongated particles fit through meshes with their smaller side. This makes for bigger particles in this fraction and thus fewer particles. Smaller particles, on the other hand, appear lighter in the recordings. Due to this it could happen that not enough contrast is given to the background to safely track one particle through multiple consecutive frames.

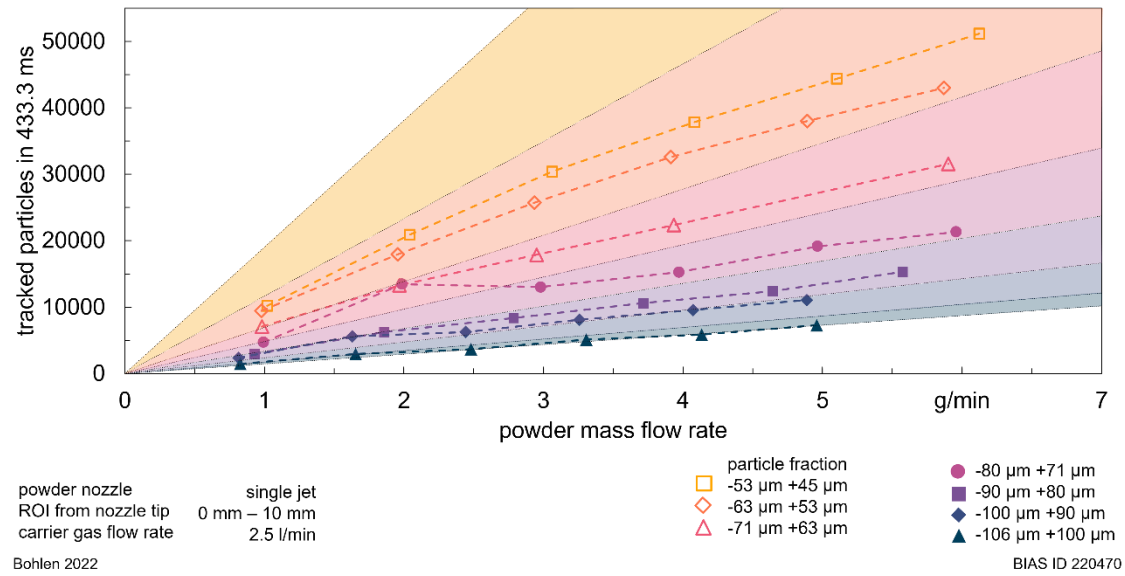

Fig. 3: Particles tracked in recordings for different powder mass flow rates.

Tracked particles for different carrier gas flow rates can be seen in Fig. 4. Overall, the particle fractions show an almost constant number of particles for different carrier gas flow rates. Exceptions are the values for the smallest amount of carrier gas (1 l/min) and for smaller particle fractions with higher carrier gas flow rates.

All particle fractions show a reduced number of particles with only 1 l/min carrier gas flow rate, this could be due to insufficient carrier gas flow. For the particle fractions -106 µm +90 µm this carrier gas flow rate was not able to transport the particles. A reduced amount of smaller tracked particles (-63 µm +45 mm) for higher carrier gas flow rates can be traced back to the analysis method where particles need be tracked through multiple consecutive frames to be taken into account.

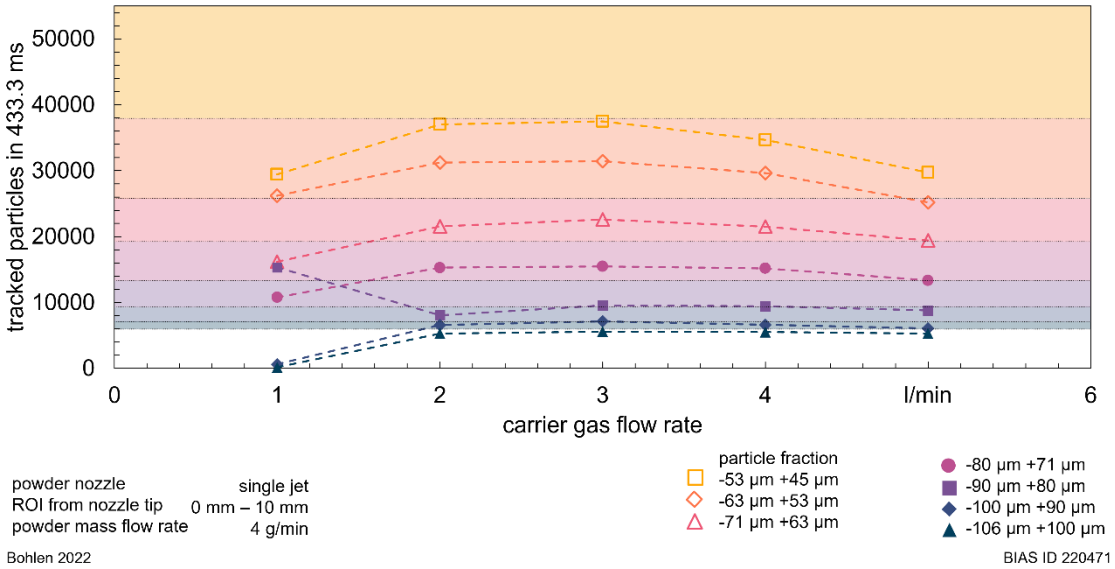

Fig. 4: Particles tracked in recordings for different carrier gas flow rates.

Calculated particle velocities for variated powder mass flow rates and variated carrier gas flow rates are shown in Fig. 5. The particle velocity remains nearly linear with in an increase of powder mass flow rate. Smaller particles (-63 mm +53 µm) show a higher velocity than larger particles (-106 µm +100 µm). An increase in carrier gas flow rate leads to an increase in particle velocity for all particle fractions as well as for the as received powder (-106 µm +45 µm).

Since the amount of particles within the powder stream is very low [3] an increase in powder mass flow rate does not lead to collisions of particles which would slow them down, leading to constant particle velocities with increasing powder mass flow rates. With a constant tube diameter for the carrier gas an increase in flow rates leads to higher gas velocities and thus to higher particle velocities. Light particles will be more accelerated by the gas flow. For both, variated powder mass flow rate and carrier gas flow rate the velocities for the as received powder is close the particle fraction -80 µm +71 µm. A possible reason for the is the high amount (49.3%) of particles in the as received powder in the range of 63 µm – 90 µm.

The divergence angle (half angle with respect to center line) of the powder after the nozzle exit can be seen in Fig. 6. An increase in powder mass flow rate leads to a decrease of divergence for all particle fractions. Smaller particles lead to a smaller divergence. For an increase in carrier gas flow rate the divergence increases, again the divergence is smaller for smaller particles.

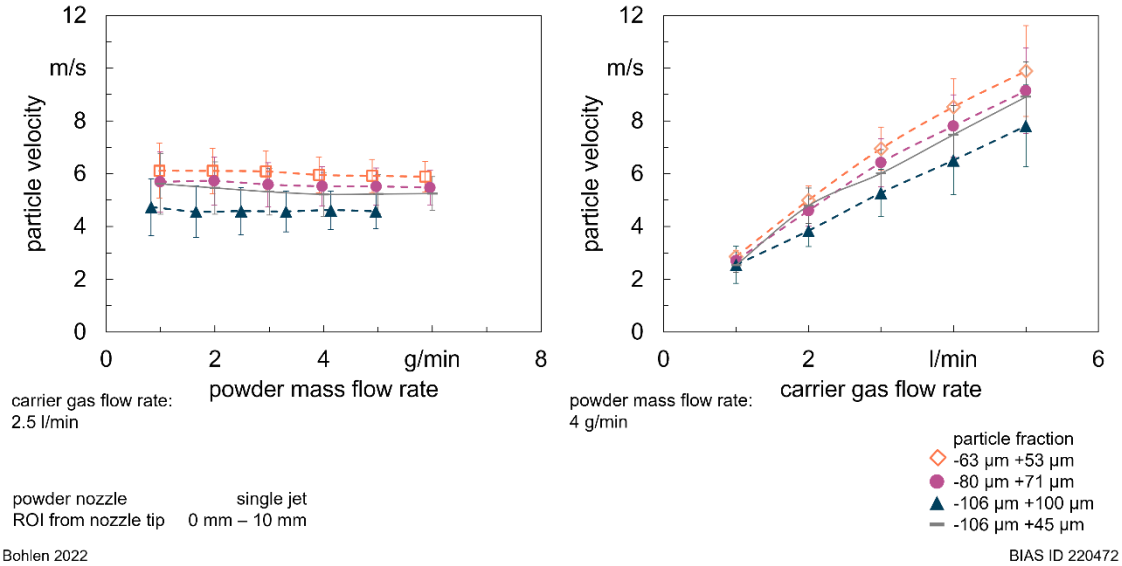

Fig. 5: Particle velocity for variated powder mass flow rate and variated carrier gas flow rates for selected particle fractions.

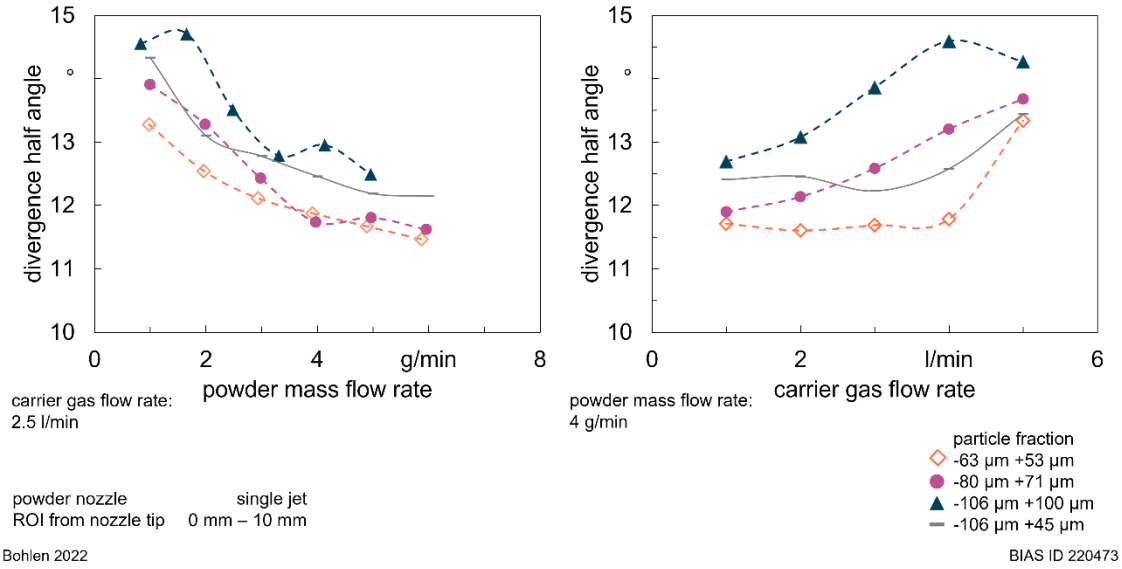

Fig. 6: Divergence angles (half angles with respect to center line) for variated powder mass flow rate and variated carrier gas flow rates for selected particle fractions.

4 Conclusion

High-speed and high-resolution imaging of the powder stream gives a detailed understanding of the influence parameters have on the powder stream. This is crucial to further improve laser metal deposition in regard to geometrical accuracy as well as improving the material utilization, making the process more economical. It is not only possible to measure the particles velocities and powder divergence but also to count single particles and tracking them through multiple frames.

Smaller particle fractions lead to an overall smaller divergence and higher particle velocities for all parameter variations.

Acknowledgements

Funded by the Deutsche Forschungsgemeinschaft (DFG, German Research Foundation) – project number 424886092 (Adaptive powder nozzle for additive manufacturing processes).

References

[1] H. Siva Prasad, F. Brueckner, A.F.H. Kaplan: Powder catchment in laser metal deposition. Journal of Laser Applications, 31 (2) (2019) 22308.
[2] J. Lin: A simple model of powder catchment in coaxial laser cladding. Optics & Laser Technology, 31 (3) (1999) 233–238.

[3] H. Tan, F. Zhang, R. Wen, J. Chen, W. Huang: Experiment study of powder flow feed behavior of laser solid forming. Optics and Lasers in Engineering, 50 (3) (2012) 391–398.
[4] S. Takemura, R. Koike, Y. Kakinuma, Y. Sato, Y. Oda: Design of powder nozzle for high resource efficiency in directed energy deposition based on computational fluid dynamics simulation. Int J Adv Manuf Technol, 105 (10) (2019) 4107–4121.
[5] P. Balu, P. Leggett, R. Kovacevic: Parametric study on a coaxial multi-material powder flow in laser-based powder deposition process. Journal of Materials Processing Technology, 212 (7) (2012) 1598–1610.
[6] I. Smurov, M. Doubenskaia, A. Zaitsev: Comprehensive analysis of laser cladding by means of optical diagnostics and numerical simulation. Surface and Coatings Technology, 220 (2013) 112–121.
[7] A. Haghshenas, A. Bohlen, D. Tyralla, R. Groll: The relevance of wall roughness modeling for simulation of powder flows in laser metal deposition nozzles. Int J Adv Manuf Technol (2022).
[8] A. Bohlen, T. Seefeld, A. Haghshenas, R. Groll: Characterization of the powder stream propagation behavior of a discrete coaxial nozzle for laser metal deposition. J. Laser Appl., 34 (2022). (in print)